A new short-term mouse model of chronic obstructive pulmonary disease identifies a role for mast cell tryptase in pathogenesis

Emma L. Beckett, B Biomed Sci,[a]* Richard L. Stevens, PhD,[b,c]* Andrew G. Jarnicki, PhD,[a]* Richard Y. Kim, B Biomed Sci,[a] Irwan Hanish, BSc,[a] Nicole G. Hansbro, PhD,[a] Andrew Deane, BSc,[a] Simon Keely, PhD,[a] Jay C. Horvat, PhD,[a] Ming Yang, MD, PhD,[a] Brian G. Oliver, PhD,[d] Nico van Rooijen, PhD,[e] Mark D. Inman, MD, PhD,[f] Roberto Adachi, MD,[g] Roy J. Soberman, MD,[b,h] Sahar Hamadi,[c] Peter A. Wark, MD, PhD,[a,i] Paul S. Foster, PhD,[a] and Philip M. Hansbro, PhD[a] *Newcastle and Sydney, Australia, Boston, Mass, Amsterdam, The Netherlands, Hamilton, Ontario, Canada, and Houston, Tex*

Background: Cigarette smoke–induced chronic obstructive pulmonary disease (COPD) is a life-threatening inflammatory disorder of the lung. The development of effective therapies for COPD has been hampered by the lack of an animal model that mimics the human disease in a short timeframe.
Objectives: We sought to create an early-onset mouse model of cigarette smoke–induced COPD that develops the hallmark features of the human condition in a short time-frame. We also sought to use this model to better understand pathogenesis and the roles of macrophages and mast cells (MCs) in patients with COPD.
Methods: Tightly controlled amounts of cigarette smoke were delivered to the airways of mice, and the development of the pathologic features of COPD was assessed. The roles of macrophages and MC tryptase in pathogenesis were evaluated by using depletion and *in vitro* studies and MC protease 6–deficient mice.
Results: After just 8 weeks of smoke exposure, wild-type mice had chronic inflammation, mucus hypersecretion, airway remodeling, emphysema, and reduced lung function. These characteristic features of COPD were glucocorticoid resistant and did not spontaneously resolve. Systemic effects on skeletal muscle and the heart and increased susceptibility to respiratory tract infections also were observed. Macrophages and tryptase-expressing MCs were required for the development of COPD. Recombinant MC tryptase induced proinflammatory responses from cultured macrophages.
Conclusion: A short-term mouse model of cigarette smoke–induced COPD was developed in which the characteristic features of the disease were induced more rapidly than in existing models. The model can be used to better understand COPD pathogenesis, and we show a requirement for macrophages and tryptase-expressing MCs. (J Allergy Clin Immunol 2013;■■■:■■■-■■■.)

Key words: *Cigarette smoke, chronic obstructive pulmonary disease, inflammation, emphysema, airway remodeling, lung function, macrophage, mast cell, protease, mouse mast cell protease 6, htryptase-β*

Cigarette smoke–induced chronic obstructive pulmonary disease (COPD) is a debilitating disorder of the lung. It is the fourth-leading cause of chronic morbidity and death worldwide, and its prevalence is increasing.[1] The disease is characterized by chronic airway inflammation, mucus hypersecretion, airway remodeling, and emphysema, which lead to reduced lung function and breathlessness.[2,3] Systemic effects also are observed in the skeletal muscle, heart, and other organs. Moreover, patients with COPD are more susceptible to respiratory tract infections. Because the mechanisms that lead to COPD and its sequelae are poorly understood at the molecular level, there are no effective treatments.

A major factor that has hampered the study of COPD is the lack of a small-animal model that recapitulates the hallmark features of the disease in a reasonable time frame. Although LPS and elastase have been used to induce lung damage in rodents that somewhat resemble COPD in human subjects, such single-factor approaches are not representative of the complex pathology that occurs in those patients who smoke for many years.[3] Current models of smoke-induced COPD involve whole-body or nose-only exposure of mice to cigarette smoke.[3] Acute models of 4 days' to 4 weeks' duration have been valuable for evaluating the early smoke-induced inflammatory responses in the lung. However, the smoke-exposed mice in these models do not have emphysema or diminished lung function.[4-8] Chronic models of more than 6 months' duration result in airway remodeling and emphysema but only induce mild alterations in lung function,[4,9-12] and the prolonged time needed to induce these features greatly restricts the use of these models for extensive therapeutic and mechanistic research. This is especially relevant considering the short lifespan of the mouse and the substantial animal and labor expenses needed for 6-month experiments. Thus there is a need

From [a]the Priority Research Centre for Asthma and Respiratory Disease and Hunter Medical Research Institute, University of Newcastle; [b]the Department of Medicine, Harvard Medical School, and [c]Brigham and Women's Hospital, Boston; [d]Sydney Medical School and Woolcock Institute of Medical Research, University of Sydney; [e]the Department of Molecular Cell Biology, Vrije Universiteit Medical Center, Amsterdam; [f]the Firestone Institute for Respiratory Health, St Joseph's Healthcare, Hamilton, Ontario; [g]the Department of Pulmonary Medicine, University of Texas MD Anderson Cancer Center, Houston; [h]Massachusetts General Hospital, Boston; and [i]the Department of Respiratory and Sleep Medicine, John Hunter Hospital, Newcastle.
*These authors contributed equally to this work.
Supported by grants from the National Health and Medical Research Council of Australia (510762, 569219, 1003565, 1003593, and 1023131), the US National Institutes of Health (AI065858 and AI059746), and the Harvard Club of Australia Foundation.
Disclosure of potential conflict of interest: R. L. Stevens has been supported by one or more grants from the National Institutes of Health. The rest of the authors declare that they have no relevant conflicts of interest.
Received for publication April 26, 2012; revised November 26, 2012; accepted for publication November 27, 2012.
Corresponding author: Philip M. Hansbro, PhD, Priority Research Centre for Asthma and Respiratory Disease and Hunter Medical Research Institute, University of Newcastle, Newcastle, NSW 2308, Australia. E-mail: Philip.Hansbro@newcastle.edu.au.
0091-6749/$36.00
© 2013 American Academy of Allergy, Asthma & Immunology
http://dx.doi.org/10.1016/j.jaci.2012.11.053

Abbreviations used

B6:	C57BL/6
BALF:	Bronchoalveolar lavage fluid
COPD:	Chronic obstructive pulmonary disease
FEV_{100}:	Forced expiratory volume in 100 ms
FRC:	Functional residual capacity
FVC:	Forced vital capacity
htryptase-β:	Human tryptase-β
MC:	Mast cell
mMCP:	Mouse mast cell protease
qPCR:	Quantitative PCR
TLC:	Total lung capacity
WT:	Wild-type

for a mouse model of cigarette smoke–induced COPD that has all of the major features of the human condition that are induced in a shorter time frame.

Although mast cells (MCs) have been casually linked to the pathogenesis of COPD, the relevant factors exocytosed from these immune cells have not been identified.[13] MC numbers are increased in inflammatory infiltrates in patients with COPD, which is associated with reduced lung function, airway remodeling, and emphysema.[14,15] MC-derived human (h)tryptase-β levels in sputum correlated with the severity of COPD in one study,[16] and the exposure of IL-3–dependent MCs to cigarette smoke–treated culture medium resulted in increased expression of mouse mast cell protease 6 (mMCP-6).[17] mMCP-6 is also known to promote inflammation, chemokine expression, and macrophage and neutrophil chemotaxis,[18] which are all hallmark features of COPD. Nevertheless, the roles of htryptase-β and mMCP-6 in COPD pathogenesis have not been investigated in depth.

Here we report the development of a mouse model of COPD in which we deliver tightly controlled amounts of cigarette smoke directly into the airways. The exposed mice exhibit the major characteristic features of COPD observed in human subjects after only 8 weeks of smoke exposure, thereby facilitating the discovery, testing, or both of the efficacy of new therapeutics. The model also enables us to elucidate the cellular, biochemical, and molecular mechanisms that underpin the pathogenesis of COPD. In that regard we now show, for the first time, detrimental roles for an MC-restricted tetramer-forming tryptase in experimental COPD.

METHODS

Additional details are described in the Methods section in this article's Online Repository at www.jacionline.org.

Smoke exposure

Wild-type (WT) BALB/c, WT C57BL/6 (B6), and mMCP-$6^{-/-}$ B6 mice[18] were used in the study. In each experiment 12 mice were simultaneously exposed to cigarette smoke (twelve 3R4F reference cigarettes [University of Kentucky, Lexington, Ky] twice per day and 5 times per week for 1 to 12 weeks) by using a custom-designed and purpose-built nose-only, directed-flow inhalation and smoke-exposure system (CH Technologies, Westwood, NJ) housed in a fume and laminar flow hood (see Fig E1 in this article's Online Repository at www.jacionline.org). Each exposure lasted 75 minutes. All experiments were approved by our institutional animal ethics committee.

Airway and lung inflammation, airway remodeling, and emphysema

Airway inflammation was assessed by means of differential enumeration of inflammatory cells in bronchoalveolar lavage fluid (BALF).[19-22] Parenchymal inflammation was assessed by counting the inflammatory cells in 10 randomized fields (×100 magnification) of whole lung sections.[23] RNA was extracted, and transcript levels were assessed by using standard real-time quantitative PCR (qPCR) assays[24] with the primers described in Table E1 in this article's Online Repository at www.jacionline.org.

Macrophage and MC numbers in lung homogenates were assessed by using flow cytometry and histochemistry.[25-27] Airway remodeling was determined by measuring the number of mucus-expressing goblet cells around the airways and by assessing airway epithelial thickening.[22,23,28-30] Emphysema was assessed by using the mean linear intercept technique, which is a standard method for assessing alveolar diameter and emphysema in mice.[28]

Lung function

Forced oscillation and forced maneuver techniques were used to assess lung function parameters.[25,31]

Glucocorticoid treatment

Dexamethasone (1 mg/kg in 50 μL of sterile water; Sigma, St Louis, Mo) was administered intranasally 3 times per week.[32] Control animals were sham treated with sterile water.

Respiratory tract infections

Mice were infected with mouse-adapted strains of *Streptococcus pneumoniae* intratracheally or influenza virus intranasally. Pathogen load was determined by using culture or plaque assays of lung homogenates, respectively.[33-36]

Macrophage and neutrophil depletion

Lung macrophages and neutrophils were depleted by means of intranasal administration of liposome-encapsulated clodronate or intraperitoneal injection of anti-Ly6G antibody (1A8; BioXCell, Lebanon, NH), respectively, 3 times per week.[25,37]

Transcript expression in tryptase-treated macrophages

B6 mouse bone marrow–derived macrophages were cultured in the absence or presence of recombinant htryptase-β (0.8 μg/mL, 25 nmol/L; Promega, Madison, Wis). RNA was isolated, and qPCR assays were used to evaluate the levels of TNF-α, Cxcl1/keratinocyte chemokine, and IL-1β transcripts.

Statistical analyses

Data are presented as means ± SEMs (n = 6-8). Comparisons between 2 groups were made by using a 2-tailed Mann-Whitney test. Multiple comparisons were made by using 1-way ANOVA with the Tukey post-test or Kruskal-Wallis analysis with the Dunn post-test, in which nonparametric analyses were appropriate. Weights were assessed by using 1-way ANOVA (repeated measures). Analyses used GraphPad Prism Software (San Diego, Calif).

RESULTS

Nose-only exposure of WT BALB/c mice to cigarette smoke induces the hallmark features of COPD

We delivered tightly controlled amounts of cigarette smoke into the nares of WT BALB/c mice for 1 to 12 weeks and assessed the hallmark features of COPD. Weight loss was evident within the first week of exposure (Fig 1, *A*). Animals lost 10% of their initial weight after 3 weeks and only regained 5% of this initial weight over the remaining exposure period. In contrast, age-matched nonexposed mice steadily gained weight. Four days of exposure to cigarette smoke led to acute inflammation in the airways characterized by increased macrophage and neutrophil numbers in the BALF (Fig 1, *B*). Inflammation persisted and increased with the additional

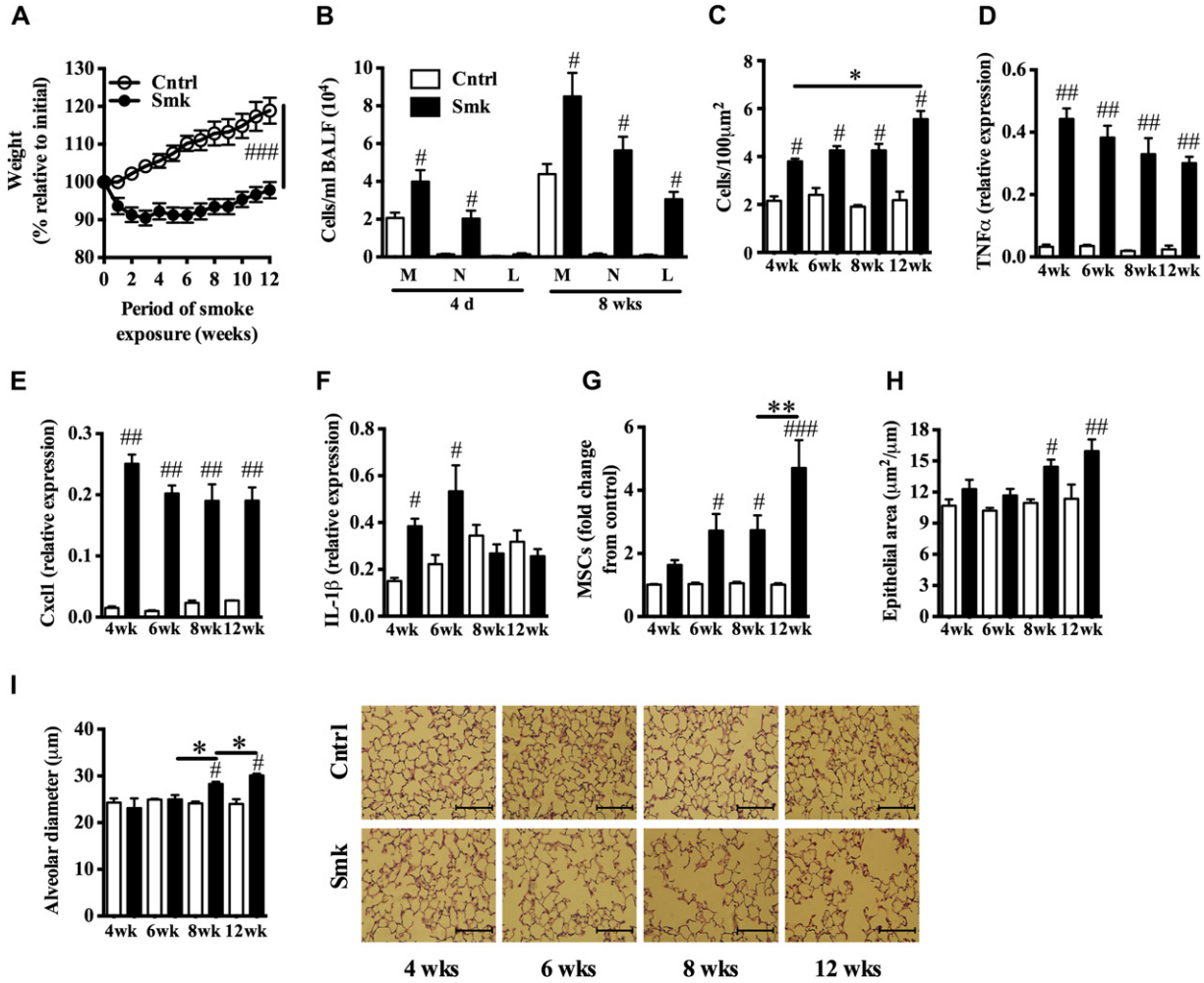

FIG 1. Nose-only exposure of the lungs of BALB/c mice to cigarette smoke induces the hallmark features of human COPD. WT BALB/c mice were exposed to cigarette smoke or normal air for 1 to 12 weeks. Relative to control mice, smoke-exposed mice had reduced weight gain relative to initial weight **(A)**; acute (after 4 days) and chronic (after 8 weeks) increases in macrophage *(M)*, neutrophil *(N)*, and lymphocyte *(L)* numbers in the BALF **(B)**; increased cellular infiltrates in the parenchyma **(C)**; increased levels of transcripts that encode TNF-α **(D)**, Cxcl1 **(E)**, and IL-1β **(F)** in lung homogenates; increased numbers of mucus-secreting goblet cells *(MSCs)* in the airways **(G)**; airway epithelial thickening **(H)**; and alveolar enlargement **(I)**. *Scale bar on micrographs* = 100 μm. Data are means ± SEMs of 6 to 8 mice per group. #$P < .05$, ##$P < .01$, and ###$P < .001$ compared with mice that breathed normal air. *$P < .05$ and **$P < .01$ compared with the other groups indicated. Statistical significance of the reduced weight gain is for the whole curve. *Cntrl*, Control; *Smk*, smoke.

involvement of lymphocytes (particularly $CD8^+$ T cells) after 8 weeks. Smoke exposure also induced progressive increases in chronic parenchymal inflammation (Fig 1, *C*). This was accompanied by increased expression in the lung of the transcripts that encode TNF-α (Fig 1, *D*), Cxcl1 (Fig 1, *E*), and IL-1β (Fig 1, *F*) but not IL-6, IL-10, IL-13, or IFN-γ (data not shown). There were signs of airway remodeling with increased numbers of mucus-secreting goblet cells in the airways from week 6 and thickening of the airway epithelium from week 8 (Fig 1, *G* and *H*). Airway remodeling was accompanied by alveolar enlargement (increases in alveolar diameter representative of emphysematous tissue destruction) after 8 weeks, which increased in severity by week 12 (Fig 1, *I*). Although there likely was a steady continuum of pathologic changes taking place in the smoke-exposed lungs of the WT mice, the results revealed the induction and progression of the disease over weeks 4 to 6 and 8 to 12, respectively.

Smoke exposure of the airways of mice resulted in reduced lung function similar to that observed in human subjects with COPD

Because 8 weeks of exposure was required to induce key features of COPD, other parameters were assessed at this time point. We next investigated the effects of smoke exposure on parameters of lung function. Exposure decreased hysteresis, transpulmonary and airway-specific resistance, tissue damping, and forced expiratory volume in 100 ms (FEV_{100})/forced vital capacity (FVC) ratio (representative of FEV_1/FVC ratio in human subjects) but increased dynamic compliance, work of breathing, functional residual capacity (FRC), and total lung capacity (TLC) (Fig 2). These adverse changes in lung function likely resulted from the combination of chronic inflammation, airway remodeling, and emphysematous lesions with associated reductions in alveolar tissue and supporting airway attachments.

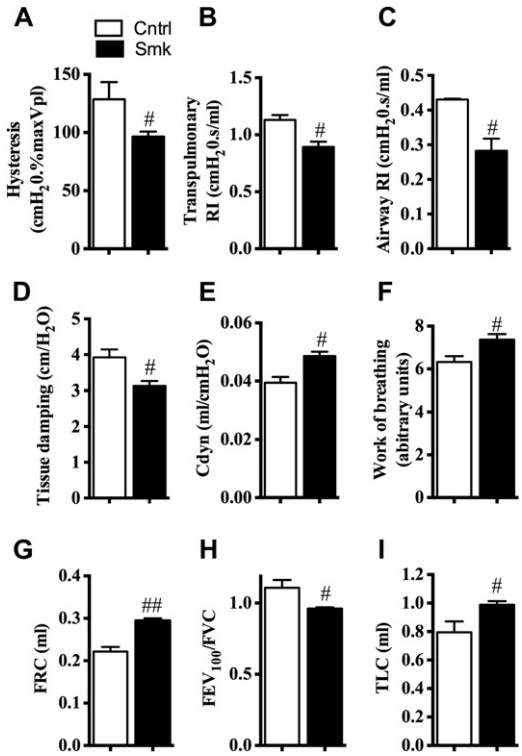

FIG 2. Nose-only cigarette smoke exposure leads to changes in lung function that are similar to those seen in human subjects with COPD. WT BALB/c mice were exposed to cigarette smoke or normal air for 8 weeks. Relative to control mice, smoke-exposed mice had decreased hysteresis **(A)**, transpulmonary **(B)** and airway-specific **(C)** resistance *(RI)*, and tissue damping **(D)** but increased dynamic compliance (*Cdyn*; **E**), work of breathing **(F)**, FRC **(G)**, and TLC **(H)** and reduced FEV_{100}/FVC ratio **(I)**. Data are means ± SEMs of 6 to 8 mice per group. #$P < .05$ compared with mice that breathed normal air. *Cntrl*, Control; *Smk*, smoke.

COPD features in the experimental model are glucocorticoid resistant

Although glucocorticoids are used to treat patients with COPD to reduce acute inflammation and the frequency of acute exacerbations,[38,39] they have limited efficacy.[40-42] Glucocorticoid treatment (either throughout or for the last 6 weeks of 12 weeks of smoke exposure) did not prevent chronic inflammation or emphysema nor did they suppress decreases in lung function (Fig 3).

Smoke exposure of the airways has systemic effects

The lung is not the only organ adversely affected in human subjects with COPD, and systemic inflammation, loss of skeletal muscle mass, and cardiovascular disease often occur in patients with this disease.[43] In our model 8 weeks of exposure also induced systemic changes, with significant alterations in the proportion of leukocytes in the blood. The percentage of monocytes decreased, but the percentage of neutrophils and lymphocytes increased (Fig 4, *A*). Furthermore, skeletal muscle mass (ie, the quadriceps) was reduced (Fig 4, *B*). Moreover, the hearts of smoke-exposed mice were enlarged by approximately 25% and had more surrounding fatty tissue (Fig 4, *C*).

Induction of experimental COPD exacerbates respiratory tract infections

Chronic microbial colonization of the airways and infection-induced exacerbations are common in patients with COPD.[44] When we infected mice previously exposed to smoke for 8 weeks with *S pneumoniae* or influenza virus (and smoke exposure discontinued), pathogen burden increased approximately 10-fold and approximately 2.5-fold, respectively (Fig 4, *D* and *E*).

Experimental COPD does not rapidly resolve after smoking cessation

Once patients have COPD, their clinical conditions generally do not improve significantly after smoking cessation, and often lung function further deteriorates.[2] In our model smoke exposure for 8 weeks followed by cessation for 4 weeks did not improve airway inflammation, emphysema, lung function, or circulating leukocyte abnormalities (Fig 5). In regard to airway inflammation (Fig 5, *A*), the numbers of macrophages continued to increase, suggesting the presence of a macrophage-rich proinflammatory environment in the lung that underpins the progression of disease.

Experimental COPD is macrophage dependent

Numerous studies have indicated that pulmonary macrophages have prominent pathologic roles in human subjects with COPD.[7,9,45,46] Because increased numbers of macrophages were found in the lungs of our smoke-exposed WT mice (Fig 1, *B*), we assessed the importance of these phagocytes in the development of experimental COPD by reducing their numbers during smoke exposure using the clodronate depletion method. Liposome-encapsulated clodronate was administered into the airways 3 times per week throughout 8 weeks of smoke exposure. Control animals were sham treated with empty liposomes. Macrophage numbers were then quantified in the BALF by using morphology and in dispersed whole lung tissue by using flow cytometry ($F4/80^+$). Macrophages were depleted by 61% ± 4% and 73% ± 5% in smoke-exposed mice and by 25% ± 3% and 36% ± 2% in nonexposed control animals in BALF and lung tissue, respectively. In contrast, the percentage of monocytes in the peripheral blood was unaffected. Macrophage depletion in the lung resulted in reduced smoke-induced epithelial thickening and emphysema and protection against alterations in lung function (Fig 6). In contrast, depletion of neutrophils with the anti-Ly6G antibody approach did not suppress the effects of smoke exposure (see Fig E2 in this article's Online Repository at www.jacionline.org). The accumulated data suggest a central role for pulmonary macrophages in our animal model of cigarette smoke–induced COPD, thereby supporting the clinical data of others that have implicated these cells in the pathogenesis of COPD in human subjects.[7]

Exposure of WT B6 mice to cigarette smoke also induces COPD

WT BALB/c and B6 mice respond differently in numerous disease models. To assess the general applicability of our model to another commonly used mouse strain, we examined the effects of smoke exposure on the lungs of WT B6 mice. Exposure for 8 weeks resulted in a similar profile and magnitude of weight loss, parenchymal inflammation, airway remodeling, emphysematous destruction (alveolar enlargement), and altered lung function in B6 mice compared with BALB/c mice (see Fig E3 in this article's Online Repository at www.jacionline.org).

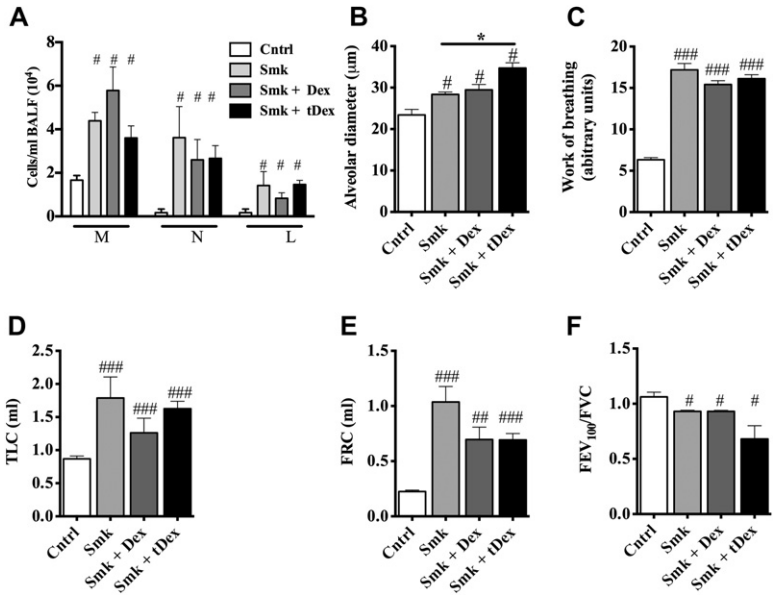

FIG 3. Experimental COPD is glucocorticoid resistant. WT BALB/c mice were exposed to cigarette smoke or normal air for 12 weeks and were treated with dexamethasone or sham-treated with sterile distilled water either prophylactically throughout *(Dex)* or therapeutically *(tDex)* for the last 6 weeks of the smoking protocol. Steroid treatment had no effect on macrophage *(M)*, neutrophil *(N)*, and lymphocyte *(L)* numbers in the BALF **(A)**; alveolar enlargement or changes in lung function **(B)**; or work of breathing **(C)**, TLC **(D)**, FRC **(E)**, or FEV_{100}/FVC ratio **(F)**. Data are means ± SEMs of 6 to 8 mice per group. #$P < .05$, ##$P < .01$, and ###$P < .001$ compared with mice that breathed normal air. *$P < .05$ compared with the other groups indicated. There were no differences between the other groups. *Cntrl*, Control; *Smk*, smoke.

The tetramer-forming tryptase mMCP-6 contributes to macrophage accumulation and inflammation in the airways and is required for experimental COPD

Macrophage accumulation in the lungs of smoke-exposed mice could be caused by unknown factors released from activated MCs. Although MCs have been implicated in the pathogenesis of COPD as well, the link between these 2 cell types and smoke-induced COPD has not been demonstrated, and the relevant MC-derived factors have not been identified.[13] After 8 weeks of smoke exposure, macrophage and MC numbers in the lungs of WT B6 mice (ie, the largest lobe in the multilobed right lung by means of flow cytometry or in the single-lobed left lung by means of histochemistry) increased approximately 3-fold in both instances (Fig 7 and see Fig E4 in this article's Online Repository at www.jacionline.org).

To provide further evidence for the importance of macrophages and MCs in pathogenesis, we also assessed their levels in smoking cessation and clodronate depletion studies. In the cessation studies the numbers of both of these cell types were increased concomitant with the maintenance of disease (Fig 7). In the depletion studies the suppression of macrophages but not MCs in the lung correlated with the prevention of COPD (Fig 7). These studies provide further evidence for the pivotal role of macrophages in the pathogenesis of experimental COPD.

mMCP-6 and htryptase-β have prominent roles in innate immunity and inflammation.[18,47] Thus we hypothesized that mMCP-6 might play a critical role in experimental COPD, as occurs in experimental arthritis and colitis. We therefore subjected WT and mMCP-$6^{-/-}$ B6 mice[18] to smoke exposure. We could not detect mMCP-6 mRNA using qPCR in the lungs of nontreated and smoke-treated WT mice, and the mMCP-6 protein levels were less than the limits of detection with SDS-PAGE immunoblot analysis. MC numbers in the lungs of smoke-exposed mMCP-$6^{-/-}$ mice were not affected and were similar to those in the lungs of smoke-exposed WT mice. However, smoke-exposed mMCP-$6^{-/-}$ mice had significantly fewer macrophages (Fig 8, *A* and *B*). The reduction in macrophage accumulation in the airways of the tryptase-deficient mice correlated with reductions in neutrophil numbers in the BALF, inflammation of the parenchyma, proinflammatory cytokine (eg, TNF-α and IL-1β) and chemokine (eg, Cxcl1) mRNA levels, and emphysematous lesions (Fig 8, *C-H*). Although airway remodeling also was abrogated, there were no obvious differences in the lung function parameters measured between smoke-treated WT and mMCP-$6^{-/-}$ mice (Fig 8, *I* and *J*). Although our accumulated data revealed adverse roles for mMCP-6 in the COPD model, other factors that remain to be identified must contribute to the deterioration in lung function in the smoke-exposed mice.

htryptase-β induces macrophages to increase their expression of proinflammatory cytokines and chemokines

To confirm the link between MC tryptases and the proinflammatory activity of activated macrophages, we next treated cultured mouse bone marrow–derived macrophages with recombinant htryptase-β. The tryptase induced these macrophages to markedly increase the levels of the transcripts that encode TNF-α, Cxcl1, and IL-1β (Fig 8, *K-M*). These changes did not occur if the tryptase was boiled for 5 minutes before treatment. Although the mechanism by which MC tetramer-forming tryptases induce macrophages to increase the expression of these cytokines and chemokines remains to be determined at the molecular level, the collective data suggest that mMCP-6 and htryptase-β are associated with macrophage accumulation and

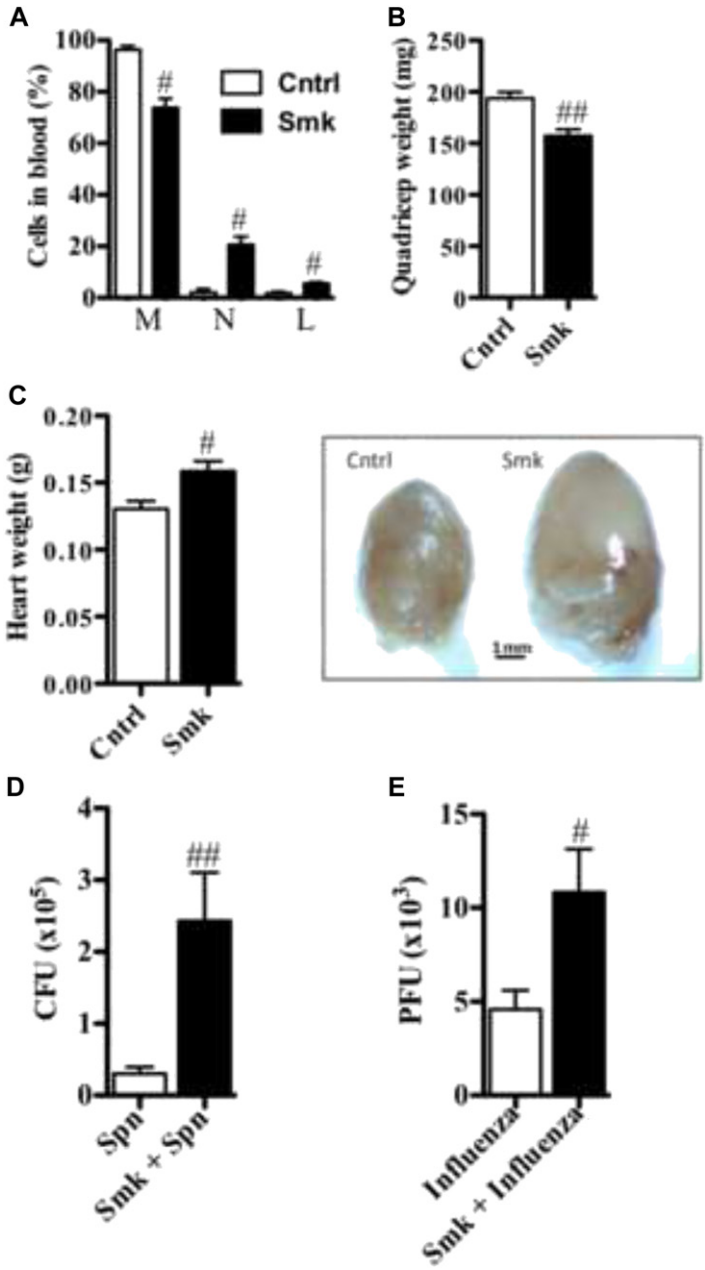

FIG 4. Experimental COPD has systemic involvement and exacerbates respiratory tract infections. WT BALB/c mice were exposed to cigarette smoke or normal air for 8 weeks. Relative to control mice, smoke-exposed mice had alterations in the proportions of monocytes (*M*; decreased), neutrophils (*N*; increased), and lymphocytes (*L*; increased) in blood **(A)**; reduced quadriceps weight **(B)**; increased heart weight, size, and fatty deposits **(C)**; and decreased clearance of *S pneumoniae* (after 48 hours of infection; **D**) and influenza virus (after 7 days of infection; **E**). Data are means ± SEMs of 6 to 8 mice per group. #$P < .05$ and ##$P < .01$ compared with WT mice that breathed normal air. *Cntrl*, Control; *Smk*, smoke.

macrophage-dependent inflammation, remodeling, and emphysema in patients with COPD.

DISCUSSION

COPD is a major respiratory health problem worldwide[2] that is usually caused by the chronic inhalation of cigarette smoke.[48,49] Although a heterogeneous disease, COPD is characterized by chronic airway inflammation (bronchitis), emphysema, or both, as well as reduced lung function.[49] The chronic inflammation that occurs in the smoke-exposed lung is thought to drive the progressive mucus hypersecretion, airway remodeling, and destruction of alveolar tissue that synergize to reduce pulmonary function.[48,49] Although inhaled glucocorticoids and bronchodilators are used therapeutically to treat the symptoms and exacerbations of COPD,[39] there is no effective treatment that prevents the induction of the disease or halts its progression.[41]

The lack of a cigarette smoke–induced animal model of COPD of short duration that recapitulates the major features of the human condition has hindered our understanding of the disease. To address

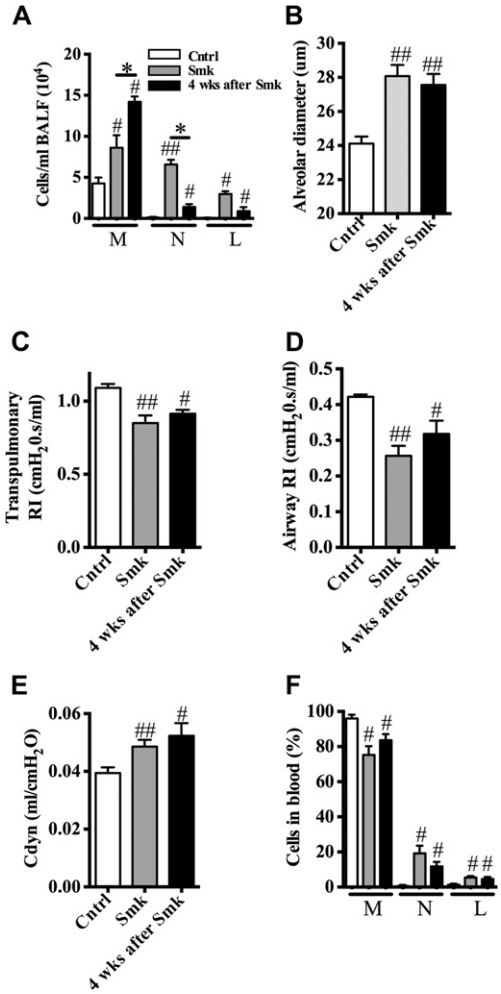

FIG 5. Experimental COPD does not rapidly resolve after cessation of smoke exposure. WT BALB/c mice were exposed to cigarette smoke or normal air for 8 weeks. Smoke-exposed mice were evaluated immediately after the cessation of smoking or 4 weeks later. Relative to control mice, both groups of smoke-exposed mice had increased airway inflammation **(A)** and alveolar enlargement **(B)**; changes in lung function; decreased transpulmonary **(C)** and airway-specific **(D)** resistance *(RI)*; increased dynamic (*Cdyn*; **E**); and altered leukocyte populations in blood **(F)**. Mice that had ceased smoking 4 weeks earlier had more macrophages but fewer neutrophils in their BALF. Data are means ± SEM of 6 to 8 mice per group. #$P < .05$ and ##$P < .01$ compared with mice that breathed normal air. *$P < .05$ compared with the other groups indicated. *Cntrl*, Control; *L*, lymphocytes; *M*, monocyte; *N*, neutrophils; *Smk*, smoke.

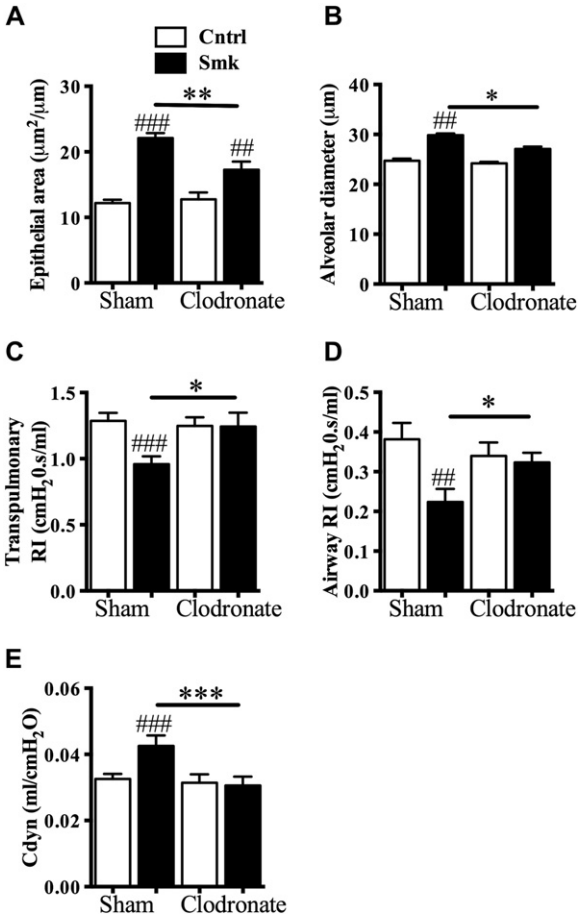

FIG 6. Depletion of pulmonary macrophages suppresses the development of experimental COPD. WT BALB/c mice were exposed to cigarette smoke or normal air for 8 weeks. These 2 groups of mice also were treated with either liposome-encapsulated clodronate or empty liposomes *(Sham)* 3 times per week for the duration of the experiment, commencing on the first day of smoking. Relative to smoke-exposed macrophage-sufficient mice, smoke-exposed macrophage-depleted mice had reduced airway epithelial thickening **(A)**, alveolar enlargement **(B)**; altered lung function; increased transpulmonary **(C)** and airway-specific **(D)** resistance *(RI)*; and reduced dynamic compliance (*Cdyn*; **E**). The smoke-exposed macrophage-depleted mice had no alveolar enlargement or changes in lung function compared with non–smoke-exposed control mice. Data are means ± SEMs of 6 to 8 mice per group. ##$P < .01$ and ###$P < .001$ compared with mice that breathed normal air. *$P < .05$, **$P < .01$, and ***$P < .001$ compared with the other groups indicated. *Cntrl*, Control; *Smk*, smoke.

this deficiency, we developed a short-term mouse model of cigarette smoke–induced COPD that has most of the key pathologic and clinical features of the human disease. Importantly, our *in vivo* model gradually progresses to overt disease over 6 to 8 weeks (Fig 1) and does not rapidly resolve (Fig 5). The hallmark features of the disease are induced within 8 weeks (Figs 1 and 2 and see Fig E3), providing opportunities to identify therapeutic targets for both the induction and progression phases of the disease. As occurs in human subjects who smoke,[14,47,50] the direct delivery of smoke to the airways of WT BALB/c and B6 mice resulted in acute and chronic inflammation that was dominated by neutrophils, macrophages, and eventually $CD8^+$ T cells (Fig 1 and see Fig E3). The disease also had an MC component (Figs 7 and 8).

Inflammation was associated with airway remodeling, emphysematous changes, and reduced lung function (Figs 1 and 2 and see Figs E2 and E3). The airway remodeling, alveolar enlargement, and emphysema were likely due to inflammation-induced damage of the parenchymal walls. Together, the airway remodeling and emphysema in our model led to reduced lung function, as occurs in human subjects with COPD (Fig 2 and see Fig E3).

The only feature not consistent with human COPD was a decrease in airway resistance (Fig 2, *B* and *C*). This finding suggests an absence of obstruction, despite the presence of goblet cell metaplasia and airway remodeling. Because mice have a greater proportion of parenchyma to airway tissue compared with human subjects, the reduced resistance might be the result of emphysema and associated reductions in tissue attachments. Alveolar distension and hyperinflation led to widening of the airways during ventilation and reduced resistance in other mouse models of emphysema.[51]

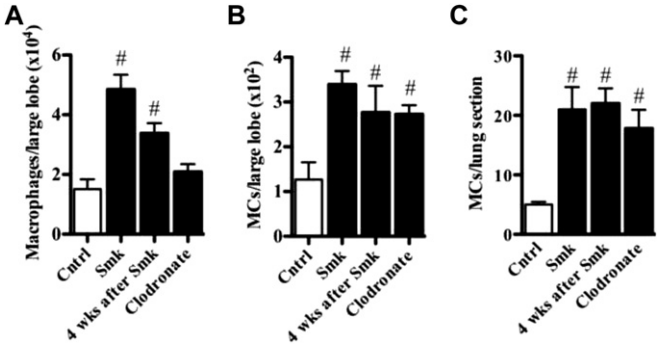

FIG 7. Experimental COPD increases the numbers of pulmonary macrophages and MCs. WT B6 mice were exposed to cigarette smoke or normal air for 8 weeks. Some mice were then rested for 4 weeks after smoking. Other mice were treated with clodronate. Relative to control mice, smoke-exposed mice had increased numbers of F4/80$^+$ macrophages **(A)** and Kit$^+$/FcεRI$^+$/IgE$^+$ cells (**B**; as determined by means of flow cytometry in the largest lobe of the multilobed right lung) or toluidine blue–positive (**C**; as determined by means of histochemistry in the single-lobed left lung) MCs in the lungs. Smoking cessation did not alter macrophage or MC numbers. Clodronate specifically attenuated macrophage numbers. Data are means ± SEMs of 6 to 8 mice per group. #P < .05 compared with mice that breathed normal air. *Cntrl*, Control; *Smk*, smoke.

Glucocorticoids have limited efficacy in treating COPD symptoms in human subjects. They partially suppress chronic inflammation but do not reverse the tissue lesions or modify factors that drive chronic disease and have no effect on the decrease in lung function.[40-42] As occurs in patients with COPD, dexamethasone did not suppress inflammation, emphysema, or alterations in lung function in our model (Fig 3). COPD has a systemic component, with changes in circulating leukocyte populations and loss of skeletal muscle mass.[43] Both of these features were observed in our model (Fig 4, *A* and *B*). COPD is also linked to cardiovascular disease, and the hearts of smoke-exposed WT mice had pathologic changes (Fig 4, *C*).

Patients with COPD have a 3- to 6-fold increased risk of *S pneumoniae*–induced pneumonia.[52] They also are more susceptible to influenza virus and have severe symptoms when infected.[53] Respiratory tract infections induce further inflammation and acute exacerbations of COPD symptoms, which, in turn, increase the rate of disease progression.[54] The development of experimental COPD was associated with enhanced respiratory tract infection by *S pneumoniae* and influenza virus (Fig 4, *D* and *E*). The numbers of CD8$^+$ T cells that infiltrated the lungs of smoke-exposed mice were increased, but these lymphocytes showed reduced expression of the activation marker CD98 (data not shown), which might contribute to impaired pathogen clearance. Although inflammation was increased, the latter findings suggest that immune function was suppressed, thereby predisposing the diseased mice to more severe pulmonary infections.

Once COPD develops in human subjects, the clinical condition and features of disease often deteriorate further, even after the cessation of smoking.[2] After 8 weeks of smoking and 4 weeks of cessation in our model, macrophage accumulation in the airways of WT mice actually increased compared with that observed immediately after 8 weeks of smoking (Fig 5, *A*). It is possible that the increase in macrophage numbers in the lungs underpins the progression of COPD, even after smoking cessation. This macrophage accumulation might be additionally exacerbated by infection that could further increase the rate of disease progression. There were no signs of resolution of any features of disease, at least 4 weeks after smoking cessation (Fig 5).

We then performed macrophage-depletion studies in WT mice to demonstrate that these phagocytes were essential for smoke-induced emphysema and reduced lung function (Fig 6). The clodronate method is the only method that can be used to reliably deplete the number of macrophages in the lungs of mice. Although clodronate might deplete some dendritic cells, there was no reduction in neutrophil numbers by using the method. Furthermore, the direct depletion of neutrophils did not suppress changes in lung structure or function (see Fig E3).

The mechanisms that drive COPD pathogenesis are incompletely understood. Chronic influx of inflammatory cells into the lungs in patients with COPD leads to the generation and release of proinflammatory cytokines, chemokines, and leukotrienes,[55] which are thought to contribute to tissue destruction and the development of COPD. However, abnormalities in the protease/protease inhibitor balance in the lung are important as well.[56] In that regard MCs and their tryptase-serglycin proteoglycan complexes promote inflammation in numerous diseases,[47,57,58] and MCs have been implicated in COPD pathogenesis.[13] MCs are common in inflammatory infiltrates in patients with COPD, and increases in their numbers correlate with reduced lung function and airway remodeling.[14] MC numbers detected in smoke-exposed mice were not high relative to numbers of other cell types (Fig 7). Nevertheless, it is well known that MCs release potent proinflammatory mediators and that even small numbers of these cells can have devastating effects *in vivo*, as occurs in systemic anaphylaxis.

htryptase-β[59,60] comprises up to 50% of the protein content of a human MC. Its ortholog, mMCP-6,[61] has beneficial roles in the control of infections[18,62] but adverse roles in MC-dependent inflammation of the airways,[53] joints,[47,57] and colon[58,63] in mice. However, the roles of MCs and their granule mediators in COPD pathogenesis have not been elucidated. In our model there were no detectable increases in mMCP-6 mRNA or protein levels. This was not surprising because MC tryptases are preformed and stored in the cell's granules. Thus changes in their mRNA levels are not as important as their release or the activation state of the MC. Only low levels of MCs were observed, and mMCP-6 protein levels were less than the limits of detection by means of immunoblotting in whole lung tissues. There are no other more sensitive tests, such as ELISA, available. Nevertheless, Mortaz et al[17] have demonstrated that cigarette smoke–conditioned media induced the expression of mMCP-6 protein in primary cultured MCs.

Despite these data, the generation of mMCP-6$^{-/-}$ B6 mice[18] allowed us the opportunity, for the first time, to definitively evaluate the importance of this MC-restricted tryptase in experimental COPD. The MCs in WT BALB/c mice express mMCP-6[61] and the other tryptase family member, mMCP-7.[64] In contrast, the MCs in WT B6 mice lack mMCP-7 because of a splice-site mutation in its gene.[65] The finding that all the features of COPD were similar in WT BALB/c (Fig 1) and B6 (see Fig E3) mice indicates that mMCP-7 is not essential in our experimental model.

Smoke exposure resulted in enhanced proinflammatory cytokine and chemokine expression (Figs 1, *D-F* and 8, *E* and *F*) and increased macrophage and MC numbers in the lungs of WT B6 mice (Fig 7). We then used our mMCP-6$^{-/-}$ B6 mice to demonstrate that the presence of this tryptase is required for smoke-induced proinflammatory cytokine and chemokine expression and accumulation of macrophages in the lung and for airway epithelial thickening and emphysematous damage (Fig 8). There

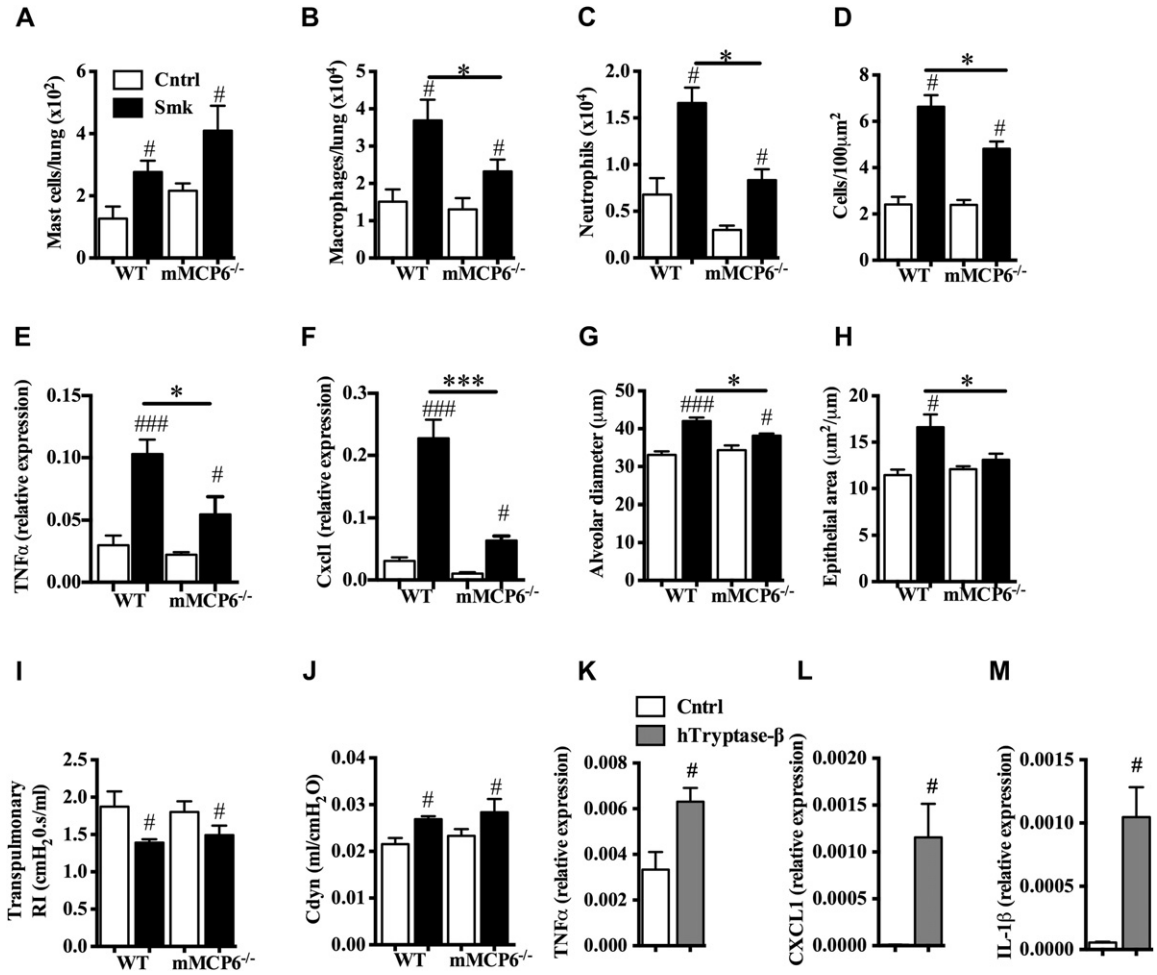

FIG 8. The tryptase mMCP-6 contributes to pulmonary macrophage accumulation and parenchymal inflammation and is required for airway remodeling and alveolar enlargement in mice with experimental COPD. **A-J,** WT and mMCP-6$^{-/-}$ B6 mice were exposed to cigarette smoke or normal air for 8 weeks. Relative to smoke-exposed WT mice, smoke-exposed mMCP-6$^{-/-}$ mice had no change in the number of Kit^{+}/FcεRI^{+}/IgE^{+} MCs (Fig 8, *A*) but had reduced numbers of F4/80^{+} macrophages (Fig 8, *B*) and neutrophils (Fig 8, *C*) in the lung, less cellular infiltrates in the parenchyma (Fig 8, *D*), attenuated TNF-α (Fig 8, *E*) and Cxcl1 (Fig 8, *F*) mRNA levels in lung homogenates, diminished alveolar enlargement (Fig 8, *G*), no airway remodeling and no differences in lung function (Fig 8, *H*; eg, transpulmonary resistance [*RI*; Fig 8, *I*] or dynamic compliance [*Cdyn*; Fig 8, *J*]). **K-M,** B6 mouse bone marrow–derived macrophages were cultured in the absence or presence of recombinant htryptase-β. Relative to untreated cells, htryptase-β–treated cells had increased levels of the transcripts that encode TNF-α (Fig 8, *K*), Cxcl1 (Fig 8, *L*), and IL-1β (Fig 8, *M*). Data are means ± SEMs of 6 to 8 mice per group or of 3 cell cultures in triplicate (representative of 4 repeat experiments). #$P < .05$ and ###$P < .001$ compared with mice that breathed normal air (Fig 8, *A-J*) or compared with sham-treated macrophages (Fig 8, *K-M*). *$P < .05$ and ***$P < .001$ compared with the other groups indicated.

were no statistically significant differences between neutrophil numbers or chemokine mRNA levels in the lung (Fig 8, *C* and *F*) or the percentage of leukocytes that were neutrophils in the blood (data not shown) at baseline. Thus the decreased cellular infiltration in the lungs of the smoke-treated mMCP-6$^{-/-}$ mice was not due to a baseline defect. We then showed that recombinant hTryptase-β induced mouse macrophages to increase their expression of the transcripts that encode the cytokines and chemokines that are increased in the lungs of mice with experimental COPD. These findings suggest the tryptase contributes to COPD, at least in part, by directly activating the macrophages in the lungs of the diseased animals. Our discovery that macrophages and tryptase-positive MCs participate in the pathogenesis of COPD in our model raises the possibility that these cells and their granule tetramer-forming tryptases have comparable adverse roles in human COPD. Thus the next generation of htryptase-β inhibitors might have efficacy in the treatment of patients with COPD.

In summary, we developed a short-term cigarette smoke–induced mouse model that has the hallmark features of COPD. This animal model enables the study of the pathogenesis of COPD in a significantly shorter timeframe than existing cigarette smoke–induced models, thereby providing opportunities for pharmacologic intervention. Our model also enables the evaluation of the consequences of COPD on the ability of the lung to combat infections. COPD is the result of a complex interplay of immune dysregulation, and our model allows the evaluation of other important parameters (eg, systemic consequences) in COPD

in the mouse. This study raises the possibility that macrophages and tryptase-positive MCs might have similar adverse roles in patients with COPD.

We thank Dr Julia Charles (Brigham and Women's Hospital, Boston, Mass) for her assistance in the generation of mouse bone marrow–derived macrophages.

Clinical implications: We describe a short-term mouse model with the hallmark features of cigarette smoke–induced COPD. We then show that the model can be used to further our understanding of the pathogenesis of COPD. We demonstrate for the first time that an MC-restricted tetramer-forming tryptase has a prominent adverse role in experimental COPD.

REFERENCES

1. World Health Organization. Global burden of disease: 2004 update. Geneva: World Health Organization; 2008.
2. Rabe KF, Hurd S, Anzueto A, Barnes PJ, Buist SA, Calverley P, et al. Global strategy for the diagnosis, management, and prevention of chronic obstructive pulmonary disease: GOLD executive summary. Am J Respir Crit Care Med 2007;176: 532-55.
3. Vlahos R, Bozinovski S, Gualano RC, Ernst M, Anderson GP. Modelling COPD in mice. Pulm Pharmacol Ther 2006;19:12-7.
4. Bracke KR, D'hulst AI, Maes T, Moerloose KB, Demedts IK, Lebecque S, et al. Cigarette smoke-induced pulmonary inflammation and emphysema are attenuated in CCR6-deficient mice. J Immunol 2006;177:4350-9.
5. Gaschler GJ, Zavitz CCJ, Bauer CMT, Skrtic M, Lindahl M, Robbins CS, et al. Cigarette smoke exposure attenuates cytokine production by mouse alveolar macrophages. Am J Respir Cell Mol Biol 2007;38:218-26.
6. Motz GT, Eppert BL, Wortham BW, Amos-Kroohs RM, Flury JL, Wesselkamper SC, et al. Chronic cigarette smoke exposure primes NK cell activation in a mouse model of chronic obstructive pulmonary disease. J Immunol 2010;184:4460-9.
7. Hodge S, Matthews G, Mukaro V, Ahern J, Shivam A, Hodge G, et al. Cigarette smoke-induced changes to alveolar macrophage phenotype and function are improved by treatment with procysteine. Am J Respir Cell Mol Biol 2011;44:673-81.
8. Atkinson JJ, Lutey BA, Suzuki Y, Toennies HM, Kelley DG, Kobayashi DK, et al. The role of matrix metalloproteinase-9 in cigarette smoke-induced emphysema. Am J Respir Crit Care Med 2011;183:876-84.
9. Hautamaki RD, Kobayashi DK, Senior RM, Shapiro SD. Requirement for macrophage elastase for cigarette smoke-induced emphysema in mice. Science 1997; 277:2002-4.
10. Wright JL, Churg A. Smoking cessation decreases the number of metaplastic secretory cells in the small airways of the guinea pig. Inhal Toxicol 2002;14:1153-9.
11. Huvenne W, Pérez-Novo CA, Derycke L, De Ruyck N, Krysko O, Maes T, et al. Different regulation of cigarette smoke induced inflammation in upper versus lower airways. Respir Res 2010;11:100-9.
12. Ruwanpura SM, McLeod L, Miller A, Jones J, Bozinovski S, Vlahos R, et al. Interleukin-6 promotes pulmonary emphysema associated with apoptosis in mice. Am J Respir Cell Mol Biol 2011;45:720-30.
13. Mortaz E, Folkerts G, Redegeld F. Mast cells and COPD. Pulm Pharmacol Ther 2011;24:367-72.
14. Andersson CK, Mori M, Bjermer L, Lofdahl CG, Erjefalt JS. Alterations in lung mast cell populations in patients with chronic obstructive pulmonary disease. Am J Respir Crit Care Med 2010;181:206-17.
15. Ballarin A, Bazzan E, Zenteno RH, Turato G, Baraldo S, Zanovello D, et al. Mast cell infiltration discriminates between histopathological phenotypes of chronic obstructive pulmonary disease. Am J Respir Crit Care Med 2012;186:233-9.
16. Zhang X, Zheng H, Ma W, Wang F, Zeng X, Liu C, et al. Tryptase enzyme activity is correlated with severity of chronic obstructive pulmonary disease. Tohoku J Exp Med 2011;224:179-87.
17. Mortaz E, Givi ME, Da Silva CA, Folkerts G, Redegeld FA. A relation between TGF-β and mast cell tryptase in experimental emphysema models. Biochim Biophys Acta 2012;1822:1154-60.
18. Thakurdas SM, Melicoff E, Sansores-Garcia L, Moreira DC, Petrova Y, Stevens RL, et al. The mast cell-restricted tryptase mMCP-6 has a critical immunoprotective role in bacterial infections. J Biol Chem 2007;282:20809-15.
19. Thorburn AN, O'Sullivan BJ, Thomas R, Kumar RK, Foster PS, Gibson PG, et al. Pneumococcal conjugate vaccine-induced regulatory T cells suppress the development of allergic airways disease. Thorax 2010;65:1053-60.
20. Essilfie AT, Simpson JL, Horvat JC, Preston JA, Dunkley ML, Foster PS, et al. *Haemophilus influenzae* infection drives IL-17-mediated neutrophilic allergic airways disease. PLoS Pathog 2011;7:e1002244.
21. Preston JA, Essilfie AT, Horvat JC, Wade MA, Beagley KW, Gibson PG, et al. Inhibition of allergic airways disease by immunomodulatory therapy with whole killed *Streptococcus pneumoniae*. Vaccine 2007;25:8154-62.
22. Thorburn AN, Foster PS, Gibson PG, Hansbro PM. *Streptococcus pneumoniae* components suppress allergic airways disease and natural killer T cells by inducing regulatory T cells. J Immunol 2012;188:4611-20.
23. Horvat JC, Beagley KW, Wade MA, Preston JA, Hansbro NG, Hickey DK, et al. Neonatal chlamydial infection induces mixed T-cell responses that drive allergic airway disease. Am J Respir Crit Care Med 2007;176:556-64.
24. Starkey MR, Essilfie AT, Horvat JC, Kim RY, Nguyen DH, Beagley KW, et al. Constitutive production of IL-13 promotes early-life *Chlamydia* respiratory infection and allergic airway disease. Mucosal Immunol 2012 [Epub ahead of print].
25. Li JJ, Wang W, Baines KJ, Bowden NA, Hansbro PM, Gibson PG, et al. IL-27/IFN-γ induce MyD88-dependent steroid-resistant airway hyperresponsiveness by inhibiting glucocorticoid signaling in macrophages. J Immunol 2010;185:4401-9.
26. Asquith KL, Horvat JC, Kaiko GE, Carey AJ, Beagley KW, Hansbro PM, et al. Interleukin-13 promotes susceptibility to chlamydial infection of the respiratory and genital tracts. PLoS Pathog 2011;7:e1001339.
27. Zhu M, Rhee I, Liu Y, Zhang W. Negative regulation of FceRI-mediated signaling and mast cell function by the adaptor protein LAX. J Biol Chem 2006;281: 18408-13.
28. Horvat JC, Starkey MR, Kim RY, Phipps S, Gibson PG, Beagley KW, et al. Early-life chlamydial lung infection enhances allergic airways disease through age-dependent differences in immunopathology. J Allergy Clin Immunol 2010;125: 617-25.
29. Horvat JC, Starkey MR, Kim RY, Beagley KW, Preston JA, Gibson PG, et al. Chlamydial respiratory infection during allergen sensitization drives neutrophilic allergic airways disease. J Immunol 2010;184:4159-69.
30. Kumar RK, Herbert C, Kasper M. Reversibility of airway inflammation and remodelling following cessation of antigenic challenge in a model of chronic asthma. Clin Exp Allergy 2004;34:1796-802.
31. Harris RS. Pressure-volume curves of the respiratory system. Respir Care 2005;50: 78-98.
32. Essilfie AT, Simpson JL, Dunkley ML, Morgan LC, Oliver BG, Gibson PG, et al. Combined *Haemophilus influenzae* respiratory infection and allergic airways disease drives chronic infection and features of neutrophilic asthma. Thorax 2012; 67:588-99.
33. Preston JA, Beagley KW, Gibson PG, Hansbro PM. Genetic background affects susceptibility in nonfatal pneumococcal bronchopneumonia. Eur Respir J 2004; 23:224-31.
34. Preston JA, Thorburn AN, Starkey MR, Beckett EL, Horvat JC, Wade MA, et al. *Streptococcus pneumoniae* infection suppresses allergic airways disease by inducing regulatory T-cells. Eur Respir J 2011;37:53-64.
35. Hsu AC, Barr I, Hansbro PM, Wark PA. Human influenza is more effective than avian influenza at antiviral suppression in airway cells. Am J Respir Cell Mol Biol 2011;44:906-13.
36. Hsu AC, Parsons K, Barr I, Lowther S, Middleton D, Hansbro PM, et al. Critical role of constitutive type I interferon response in bronchial epithelial cell to influenza infection. PLoS One 2012;7:e32947.
37. Daley JM, Thomay AA, Connolly MD, Reichner JS, Albina JE. Use of Ly6G-specific monoclonal antibody to deplete neutrophils in mice. J Leukoc Biol 2008;83:64-70.
38. Singh S, Amin AV, Loke YK. Long-term use of inhaled corticosteroids and the risk of pneumonia in chronic obstructive pulmonary disease: a meta-analysis. Arch Intern Med 2009;169:21929.
39. Calverley PM, Anderson JA, Celli B, Ferguson GT, Jenkins C, Jones PW, et al. Salmeterol and fluticasone propionate and survival in chronic obstructive pulmonary disease. N Engl J Med 2007;356:775-89.
40. Séguin RM, Ferrari N. Emerging oligonucleotide therapies for asthma and chronic obstructive pulmonary disease. Expert Opin Investig Drugs 2009;18:1505-17.
41. Yang IA, Fong KM, Sim EH, Black PN, Lasserson TJ. Inhaled corticosteroids for stable chronic obstructive pulmonary disease. Cochrane Database Syst Rev 2007; (2):CD002991.
42. Barnes PJ. Glucocorticosteroids: current and future directions. Br J Pharmacol 2011;163:29-43.
43. Barnes PJ, Celli BR. Systemic manifestations and comorbidities of COPD. Eur Respir J 2009;33:1165-85.
44. Miravitlles M, Marín A, Monsó E, Vilà S, de la Roza C, Hervás R, et al. Colour of sputum is a marker for bacterial colonisation in chronic obstructive pulmonary disease. Respir Res 2010;11:58-67.

45. Morris DG, Huang X, Kaminski N, Wang Y, Shapiro SD, Dolganov G, et al. Loss of integrin $\alpha_v\beta_6$-mediated TGF-β activation causes MMP12-dependent emphysema. Nature 2003;422:169-73.
46. Ofulue AF, Ko M, Abboud RT. Time course of neutrophil and macrophage elastinolytic activities in cigarette smoke-induced emphysema. Am J Physiol Lung Cell Mol Physiol 1998;275:L1134-44.
47. McNeil HP, Shin K, Campbell IK, Wicks IP, Adachi R, Lee DM, et al. The mouse mast cell-restricted tetramer-forming tryptases mouse mast cell protease 6 and mouse mast cell protease 7 are critical mediators in inflammatory arthritis. Arthritis Rheum 2008;58:2338-46.
48. Houghton AM, Mouded M, Shapiro SD. Common origins of lung cancer and COPD. Nat Med 2008;14:1023-4.
49. Hogg JC. Pathophysiology of airflow limitation in chronic obstructive pulmonary disease. Lancet 2004;364:709-21.
50. Battaglia S, Mauad T, van Schadewijk AM, Vignola AM, Rabe KF, Bellia V, et al. Differential distribution of inflammatory cells in large and small airways in smokers. J Clin Pathol 2007;60:907-11.
51. Vanoirbeek JA, Rinaldi M, De Vooght V, Haenen S, Bobic S, Gayan-Ramirez G, et al. Noninvasive and invasive pulmonary function in mouse models of obstructive and restrictive respiratory diseases. Am J Respir Cell Mol Biol 2010;42:96-104.
52. Welte T, Köhnlein T. Global and local epidemiology of community-acquired pneumonia: the experience of the CAPNETZ Network. Semin Respir Crit Care Med 2009;30:127-35.
53. Seemungal T, Harper-Owen R, Bhowmik A, Moric I, Sanderson G, Message S, et al. Respiratory viruses, symptoms, and inflammatory markers in acute exacerbations and stable chronic obstructive pulmonary disease. Am J Respir Crit Care Med 2001;164:1618-23.
54. Wilkinson TM, Patel IS, Wilks M, Donaldson GC, Wedzicha JA. Airway bacterial load and FEV_1 decline in patients with chronic obstructive pulmonary disease. Am J Respir Crit Care Med 2003;167:1090-5.
55. Keatings VM, Collins PD, Scott DM, Barnes PJ. Differences in interleukin-8 and tumor necrosis factor-α in induced sputum from patients with chronic obstructive pulmonary disease or asthma. Am J Respir Crit Care Med 1996;153:530-4.
56. Keely S, Talley NJ, Hansbro PM. Pulmonary-intestinal crosstalk in mucosal inflammatory disease. Mucosal Immunol 2012;5:7-18.
57. Shin K, Nigrovic PA, Crish J, Boilard E, McNeil HP, Larabee KS, et al. Mast cells contribute to autoimmune inflammatory arthritis via their tryptase/heparin complexes. J Immunol 2009;182:647-56.
58. Hamilton MJ, Sinnamon MJ, Lyng GD, Glickman JN, Wang X, Xing W, et al. Essential role for mast cell tryptase in acute experimental colitis. Proc Natl Acad Sci U S A 2011;108:290-5.
59. Schwartz LB, Lewis RA, Austen KF. Tryptase from human pulmonary mast cells. Purification and characterization. J Biol Chem 1981;256:11939-43.
60. Miller JS, Moxley G, Schwartz LB. Cloning and characterization of a second complementary DNA for human tryptase. J Clin Invest 1990;86:864-70.
61. Reynolds DS, Stevens RL, Lane WS, Carr MH, Austen KF, Serafin WE. Different mouse mast cell populations express various combinations of at least six distinct mast cell serine proteases. Proc Natl Acad Sci U S A 1990;87:3230-4.
62. Shin K, Watts GF, Oettgen HC, Friend DS, Pemberton AD, Gurish MF, et al. Mouse mast cell tryptase mMCP-6 is a critical link between adaptive and innate immunity in the chronic phase of *Trichinella spiralis* infection. J Immunol 2008;180:4885-91.
63. Oh SW, Pae CI, Lee DK, Jones F, Chiang GK, Kim HO, et al. Tryptase inhibition blocks airway inflammation in a mouse asthma model. J Immunol 2002;168:1992-2000.
64. McNeil HP, Reynolds DS, Schiller V, Ghildyal N, Gurley DS, Austen KF, et al. Isolation, characterization, and transcription of the gene encoding mouse mast cell protease 7. Proc Natl Acad Sci U S A 1992;89:11174-8.
65. Hunt JE, Stevens RL, Austen KF, Zhang J, Xia Z, Ghildyal N. Natural disruption of the mouse mast cell protease 7 gene in the C57BL/6 mouse. J Biol Chem 1996;271:2851-5.

METHODS

Mice

All mice were female and 6 to 8 weeks of age at the commencement of each experiment. mMCP-6$^{-/-}$ B6 mice were previously described.[E1] WT and mMCP-6$^{-/-}$ mice were housed in the same animal facility at the University of Newcastle. All mice received the same diets. Mice were killed by means of intraperitoneal sodium pentobarbital overdose. All animal experiments were approved by the animal ethics committee of the University of Newcastle.

Smoke exposure

Nose-only exposure was achieved by using specialized containment tubes that delivered smoke and normal air directly to the animal's nose. This protocol allowed a more intensive delivery of smoke than whole-body exposure systems. For the first 2 days, mice were exposed to 1 session of smoking with 12 puffs from each cigarette to allow acclimatization. Smoke was delivered in 2-second puffs, with 30 seconds of normal air between each puff. After day 2, the mice were subjected to 2 sessions in which they were exposed to the smoke from 12 cigarettes (morning and afternoon, separated by a recovery period). Despite the intensive exposure, no deaths caused by acute toxicity were observed. Age-matched control mice breathed normal air for the same periods of time (ie, 4, 6, 8, or 12 weeks). The dose of smoke was determined by performing acute (4 days) dose-response experiments using different levels of smoke exposure. The dose selected induced acute neutrophilic inflammation without inducing overt toxicity in exposed mice.

Airway and lung inflammation

Airway inflammation was assessed by staining cytospin preparations of cells in BALF (two 0.8-mL washes with PBS) with May-Grunwald-Giemsa and then enumeration of the different inflammatory cell types by using light microscopy, as previously described.[E2-E4] Total cell numbers were determined (cells per milliliter) by using Trypan blue staining and a hemocytometer. Parenchymal inflammation was assessed by using hematoxylin and eosin staining and counting the inflammatory cells in 10 randomized fields (selected from a pool of 50, ×100 magnification).[E5] The results for the 10 fields were averaged to produce the results for each mouse.

Transcript expression in the lung

Single-cell suspensions of whole lungs were digested with collagenase D and homogenized by using a gentleMACS Dissociator (Miltenyi Biotec, Sydney, Australia). Total RNA was extracted from homogenized lungs with Trizol Reagent (Invitrogen, Life Technologies, Paisley, United Kingdom), and first-strand cDNA was synthesized with oligo(dT)-primed reverse transcription with Superscript II (Invitrogen), according to the manufacturer's instructions.[E6] Real-time qPCR assays were performed with SYBR Green Supermix (KAPA Biosystems, Tharburton, Australia) and a ViiA7 thermal cycler (Life Technologies, Carlsbad, Calif). mRNA levels were normalized to that of the transcript that encodes the housekeeping protein hypoxanthine-guanine phosphoribosyl transferase.[E6] The primers used in these qPCR assays are listed in Table E1.

Airway remodeling

The thickness of the airway epithelium was calculated by measuring the difference between the area encompassing the epithelial cell basement membrane and lumen and was expressed as the epithelial area. Measurements were obtained with Image Pro Plus. The numbers of mucus-positive goblet cells around the airways were determined and expressed as a percentage change from that seen in control mice.[E4-E7] This prevents the size of the airways from affecting the results. Only whole, round, noncartilaginous airways were selected to prevent the angle of cut producing spurious results.[E8] These analyses were conducted in a blinded fashion.

Emphysema

Emphysema was assessed by using the mean linear intercept technique.[E6] After exsanguination, lungs were perfused with 0.9% saline at a pressure of 40 cm H_2O for 60 seconds to remove excess blood from the pulmonary capillary bed. The trachea was cannulated with a blunted 19-gauge needle. The lungs were then gently inflated with 10% buffered formalin (1 mL) and then immersed in 10% buffered formalin. Fixed-volume inflation was chosen because it has been shown to maintain lung architecture and simultaneously prevents overinflation of the lung, which would artificially enhance any increase in alveolar size in mice with signs of emphysema.[E9] Lungs were embedded in paraffin, and 5-μm sections were stained with hematoxylin and eosin for histologic analysis. Fifty randomized photomicrographs from 3 stained sections per mouse were obtained with a light microscope and digital camera linked to image analysis software (Image Pro Plus, version 6.0). The first 10 randomly selected photos that were free of cutting artifacts, compression, large airways, or blood vessels were used for analysis. An 11-horizontal-line overlay was applied to each image, and the average alveolar diameter was calculated by dividing the total length of these lines by the number of alveolar wall intercepts. The results from each of the 10 photomicrographs that were counted were then averaged to give a result per mouse. All histologic analyses were conducted in a blinded fashion.

Lung function

Mice were anesthetized with ketamine (100 mg/kg) and xylazine (10 mg/kg). They were then cannulated (tracheostomy with ligation).[E4,E5,E10] The flexiVent apparatus (Legacy System; SCIREQ, Montreal, Canada) was used to assess hysteresis, transpulmonary resistance and compliance, tissue damping, and airway-specific resistance at baseline (by using a tidal volume of 8 mL/kg at a respiratory rate of 450 breaths/min). This combination of anesthesia and ventilation is common and recommended by the manufacturer.[E11,E12] Maximal pressure-volume loops were used to calculate hysteresis.[E13] Transpulmonary resistance and dynamic compliance were assessed by using the snapshot perturbation function. The forced oscillation perturbation was then used to determine the airway's (Newtonian) resistance and tissue damping. For all perturbations, a coefficient of determination of 0.95 was the minimum allowable for an acceptable measurement. Each perturbation was conducted 3 times per animal, and the average was calculated, with a minimum ventilation period of 20 seconds allowed between each perturbation. Work of breathing, FRC, TLC, FEV_{100}, and FVC were measured by using a forced pulmonary maneuver system (Buxco, Wilmington, NC). An average breathing frequency of 150 breaths/min was applied to anesthetized animals. Work of breathing and TLC were determined by using the quasistatic pressure-volume loop, FRC was determined by using the Boyles Law FRC maneuver, and FEV_{100} and FVC were calculated by using the fast-flow maneuver. Each maneuver was performed a minimum of 3 times, and the average was calculated.

Respiratory tract infections

Mice were infected with mouse-adapted strains of *S pneumoniae* (2×10^6 colony-forming units administered intratracheally, D39 strain, serotype 2) or influenza virus (8 plaque-forming units administered intranasally, A/PR/8 H1N1 strain). Whole lungs were homogenized, and pathogen loads in colony-forming units or plaque-forming units were determined by means of culture plating and enumeration[E14,E15] or plaque assay,[E16,E17] respectively. For intratracheal administration, mice were anesthetized with 10 mg/kg Alfaxan through the intravenous route. For intranasal administration, mice were anesthetized with inhaled gaseous isoflurane (3% to 5%).

Macrophage depletion

Clodronate was a gift from Roche Diagnostics GmbH (Mannheim, Germany).[E11] It was encapsulated in liposomes by using phosphatidylcholine (LIPOID E PC; Lipoid GmbH, Ludwigshafen, Germany) and cholesterol (Sigma Chemicals, Sydney, Australia). The resulting preparations were stored under nitrogen gas, and 50-μL aliquots were administered intranasally after achievement of anesthesia to each animal 3 times per week. Sham-inoculated mice received empty liposomes.

Neutrophil depletion

Neutrophils were depleted by means of intraperitoneal injection of anti-Ly6G antibody (500 μg, 1A8; BioXCell) administered in 200 μL of saline 3 times per week for the duration of smoke exposure.[E18] Sham control mice received isotype antibody (IgG_{2A}, 2A39, BioXCell).

Flow cytometric analysis for macrophages, MCs, and neutrophils

Macrophages, MCs, and neutrophils were identified based on their surface expression of the F4/80/Emr1 antigen, Kit/CD117/FcεRI/IgE, and CD11b/Gr-1, respectively.[E11,E18,E19] The antibodies used in these immunohistochemistry assays were obtained from BioLegend (San Diego, Calf). Total cell numbers in homogenates of single lung lobes were enumerated by using Trypan blue staining and a hemocytometer. The obtained data were then used to convert the percentage populations identified by means of flow cytometry to the numbers of cells per large lung lobe.

MC immunohistochemistry

Paraffin-embedded tissue sections were mounted on glass slides. Slides were deparaffinized through a series of xylene and ethanol washes and then hydrated with distilled water. Slides were treated with toluidine blue (0.1% in 1% NaCl, Sigma) for 2.5 minutes. They were rinsed in distilled water 3 times, dehydrated quickly through 95% and absolute alcohol, exposed to xylene, and placed under cover slips. Metrochromatically stained cells were enumerated in sections of the largest lobe of the multilobed lung (n = 6-8 per group).[E20]

SDS-PAGE immunoblot analysis of mMCP-6 protein

Protein lysates were prepared from frozen lung tissues, which were homogenized in radio-immunoprecipitation assay (Sigma) lysis buffer supplemented with complete mini protease inhibitor tablets and PhosStop phosphatase inhibitor tablets (Roche, Indianapolis, Ind). Lysates were cleared of debris and concentrated by means of centrifugation (40 minutes, 3000*g*, Amicon Ultra 4, 10,000 d molecular weight cut-off; Millipore, Temecula, Calif). The soluble proteins were separated by using 12.5% SDS-PAGE and then transferred to a polyvinylidene difluoride membrane with a wet transfer system (Mini Trans-Blot Cell; Bio-Rad Laboratories, Hercules, Calif). The resulting membrane was blocked (5% BSA, Sigma) and then incubated with rat anti–mMCP-6 mAb MAB3736 (R&D Systems, Minneapolis, Minn), followed by horseradish peroxidase–conjugated anti-rat IgG antibody HAF005 (R&D Systems). Immunoreactive mMCP-6 was visualized by using enhanced chemiluminescence (ChemiDoc, Bio-Rad Laboratories).

Transcript expression in tryptase-treated macrophages

Primary nontransformed macrophages were generated by culturing B6 mouse bone marrow cells for 7 days in α-modified essential medium (Gibco/Life Technologies–Invitrogen, Carlsbad, Calif) supplemented with ribonucleosides, penicillin, streptomycin, 10% heat-inactivated FCS (Hyclone Laboratories, Logan, Utah), and 10% conditioned medium obtained from the mouse macrophage colony-stimulating factor–expressing cell line CMG14-12.[E21,E22] Before each experiment, the conditioned medium was removed, and the resulting plastic-adherent macrophages in each 12-well plate (approximately 100,000 macrophages per well) were cultured for an additional 18 hours in fresh medium containing 1% FCS (rather than 10% FCS) in the absence or presence of recombinant htryptase-β (0.8 μg/mL, 25 nmol/L, Promega). The RNeasy mini kits (Qiagen, Hilden, Germany) were used to isolate RNA, which was then converted into cDNA by using iScript cDNA synthesis kits (Bio-Rad Laboratories, Hercules, Calif). Using Qiagen's validated primer sets and a Stratagene Mx3000P system (Stratagene, La Jolla, Calif), qPCR assays were used to evaluate the levels of the transcripts that encode TNF-α, Cxcl1/keratinocyte chemokine, and IL-1β. The transcript that encodes glyceraldehyde-3-phosphate dehydrogenase was used as the positive reference control. All qPCR assays were performed with SYBR green reagents.

REFERENCES

E1. Thakurdas SM, Melicoff E, Sansores-Garcia L, Moreira DC, Petrova Y, Stevens RL, et al. The mast cell-restricted tryptase mMCP-6 has a critical immunoprotective role in bacterial infections. J Biol Chem 2007;282:20809-15.
E2. Thorburn AN, O'Sullivan BJ, Thomas R, Kumar RK, Foster PS, Gibson PG, et al. Pneumococcal conjugate vaccine-induced regulatory T cells suppress the development of allergic airways disease. Thorax 2010;65:1053-60.
E3. Essilfie AT, Simpson JL, Horvat JC, Preston JA, Dunkley ML, Foster PS, et al. *Haemophilus influenzae* infection drives IL-17-mediated neutrophilic allergic airways disease. PLoS Pathog 2011;7:e1002244.
E4. Thorburn AN, Foster PS, Gibson PG, Hansbro PM. *Streptococcus pneumoniae* components suppress allergic airways disease and natural killer T cells by inducing regulatory T cells. J Immunol 2012;188:4611-20.
E5. Horvat JC, Beagley KW, Wade MA, Preston JA, Hansbro NG, Hickey DK, et al. Neonatal chlamydial infection induces mixed T-cell responses that drive allergic airway disease. Am J Respir Crit Care Med 2007;176:556-64.
E6. Horvat JC, Starkey MR, Kim RY, Phipps S, Gibson PG, Beagley KW, et al. Early-life chlamydial lung infection enhances allergic airways disease through age-dependent differences in immunopathology. J Allergy Clin Immunol 2010;125:617-25.
E7. Kumar RK, Herbert C, Kasper M. Reversibility of airway inflammation and remodelling following cessation of antigenic challenge in a model of chronic asthma. Clin Exp Allergy 2004;34:1796-802.
E8. O'Reilly M, Hooper SB, Allison BJ, Flecknoe SJ, Snibson K, Harding R, et al. Persistent bronchiolar remodeling following brief ventilation of the very immature ovine lung. Am J Physiol Lung Cell Mol Physiol 2009;297:L992-1001.
E9. Braber S, Verheijden KA, Henricks PA, Kraneveld AD, Folkerts G. A comparison of fixation methods on lung morphology in a murine model of emphysema. Am J Physiol Lung Cell Mol Physiol 2010;299:L843-51.
E10. Preston JA, Essilfie AT, Horvat JC, Wade MA, Beagley KW, Gibson PG, et al. Inhibition of allergic airways disease by immunomodulatory therapy with whole killed *Streptococcus pneumoniae*. Vaccine 2007;25:8154-62.
E11. Li JJ, Wang W, Baines KJ, Bowden NA, Hansbro PM, Gibson PG, et al. IL-27/IFN-γ induce MyD88-dependent steroid-resistant airway hyperresponsiveness by inhibiting glucocorticoid signaling in macrophages. J Immunol 2010;185:4401-9.
E12. Harris RS. Pressure-volume curves of the respiratory system. Respir Care 2005;50:78-98.
E13. Bedoret D, Wallemacq H, Marichal T, Desmet C, Quesada Calvo F, Henry E, et al. Lung interstitial macrophages alter dendritic cell functions to prevent airway allergy in mice. J Clin Invest 2009;119:3723-38.
E14. Preston JA, Beagley KW, Gibson PG, Hansbro PM. Genetic background affects susceptibility in nonfatal pneumococcal bronchopneumonia. Eur Respir J 2004;23:224-31.
E15. Preston JA, Thorburn AN, Starkey MR, Beckett EL, Horvat JC, Wade MA, et al. *Streptococcus pneumoniae* infection suppresses allergic airways disease by inducing regulatory T-cells. Eur Respir J 2011;37:53-64.
E16. Hsu AC, Barr I, Hansbro PM, Wark PA. Human influenza is more effective than avian influenza at antiviral suppression in airway cells. Am J Respir Cell Mol Biol 2011;44:906-13.
E17. Hsu AC, Parsons K, Barr I, Lowther S, Middleton D, Hansbro PM, et al. Critical role of constitutive type I interferon response in bronchial epithelial cell to influenza infection. PLoS One 2012;7:e32947.
E18. Daley JM, Thomay AA, Connolly MD, Reichner JS, Albina JE. Use of Ly6G-specific monoclonal antibody to deplete neutrophils in mice. J Leukoc Biol 2008;83:64-70.
E19. Asquith KL, Horvat JC, Kaiko GE, Carey AJ, Beagley KW, Hansbro PM, et al. Interleukin-13 promotes susceptibility to chlamydial infection of the respiratory and genital tracts. PLoS Pathog 2011;7:e1001339.
E20. Zhu M, Rhee I, Liu Y, Zhang W. Negative regulation of FcεRI-mediated signaling and mast cell function by the adaptor protein LAX. J Biol Chem 2006;281:18408-13.
E21. Warren MK, Vogel SN. Bone marrow-derived macrophages: development and regulation of differentiation markers by colony-stimulating factor and interferons. J Immunol 1985;134:982-9.
E22. Takeshita S, Kaji K, Kudo A. Identification and characterization of the new osteoclast progenitor with macrophage phenotypes being able to differentiate into mature osteoclasts. J Bone Miner Res 2000;15:1477-88.

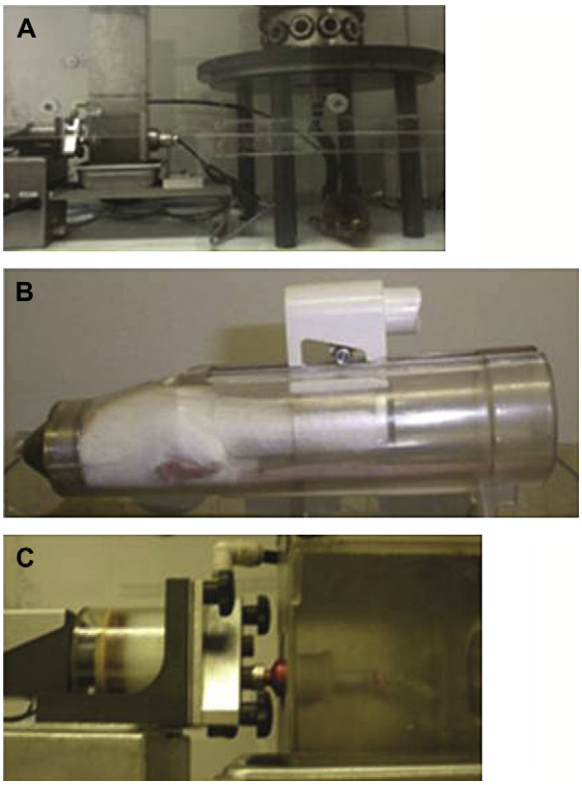

FIG E1. Custom-designed and purpose-built directed flow inhalation and smoke-exposure system. **A,** Smoking apparatus. **B,** A mouse in one of the smoking chambers. **C,** Smoking cigarette.

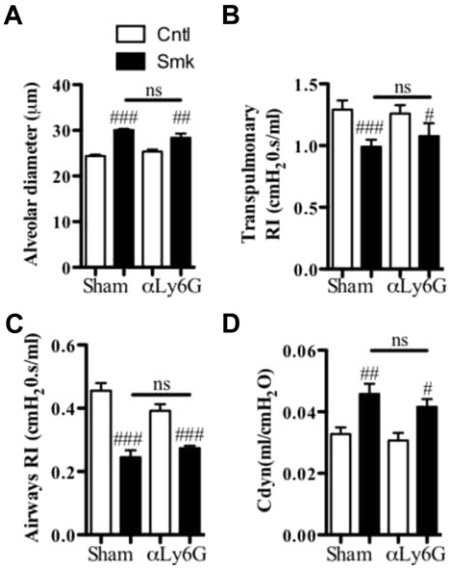

FIG E2. Depletion of pulmonary neutrophils does not suppress the development of experimental COPD. WT BALB/c mice were exposed to cigarette smoke or normal air for 8 weeks. The 2 groups of mice also were treated with either anti-Ly6G antibody or isotype control antibody *(Sham)* 3 times per week for the duration of the experiment, commencing on the first day of smoking. Relative to smoke-exposed macrophage-sufficient mice, neutrophil depletion had no effect on alveolar enlargement or alterations in lung function **(A)**, transpulmonary **(B)** or airway-specific **(C)** resistance *(RI)*, or dynamic compliance (*Cdyn*; **D**). Data are means ± SEMs of 6 to 8 mice per group. ##$P < .01$ and ###$P < .001$ compared with mice that breathed normal air. *ns*, Not significant.

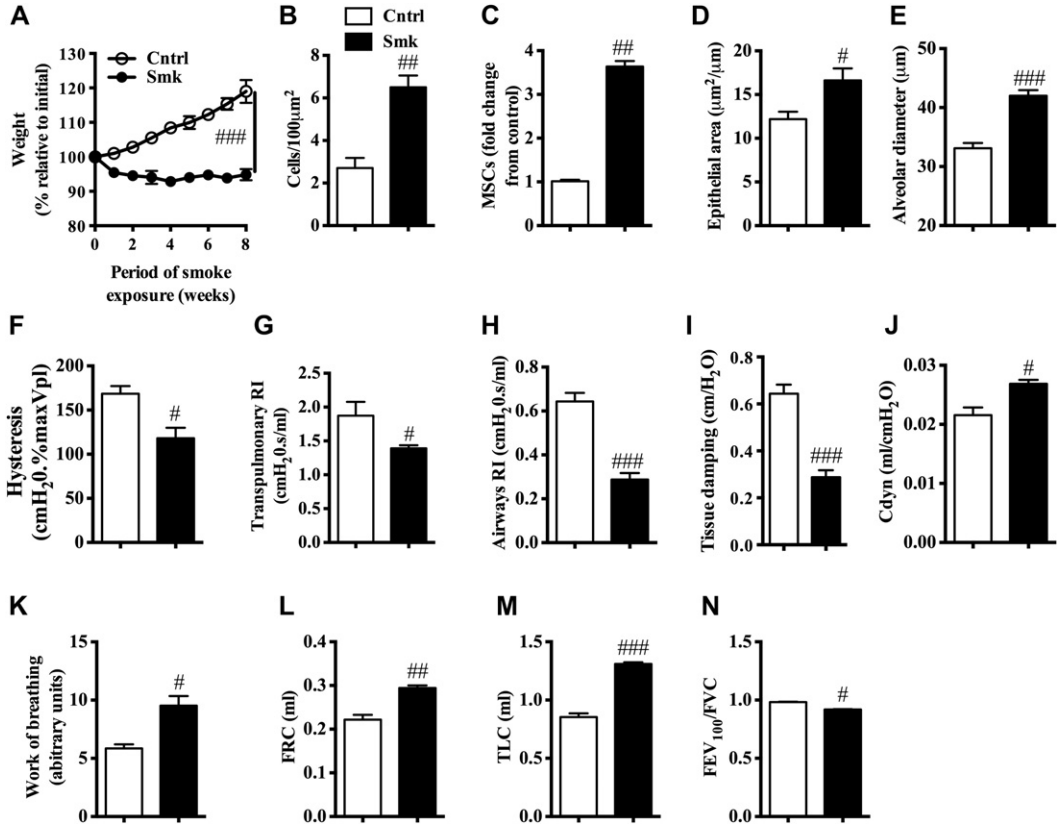

FIG E3. Nose-only exposure of WT B6 mice to cigarette smoke induces the hallmark features of human COPD. WT B6 mice were exposed to cigarette smoke or normal air for 8 weeks. Relative to control mice, smoke-exposed mice had reduced weight gain relative to initial weight **(A)**; increased cellular infiltrates in the parenchyma **(B)** and number of mucus-secreting goblet cells (*MSCs*; **C**) around the airways; airway epithelial thickening **(D)**; alveolar enlargement **(E)**; reduced lung function; decreased hysteresis **(F)**, transpulmonary **(G)** and airway **(H)** resistance *(RI)* and tissue damping **(I)**; increased dynamic compliance (*Cdyn*; **J**) and difficulty breathing **(K)**, FRC **(L)**, and TLC **(M)**; and reduced FEV_{100}/FVC ratio **(N)**. Data are means ± SEMs of 6 to 8 mice per group. #$P < .05$, ##$P < .01$, and ###$P < .001$ compared with mice that received normal air. Statistical significance of the reduced weight gain is for the whole curve. *Cntrl*, Control; *Smk*, smoke.

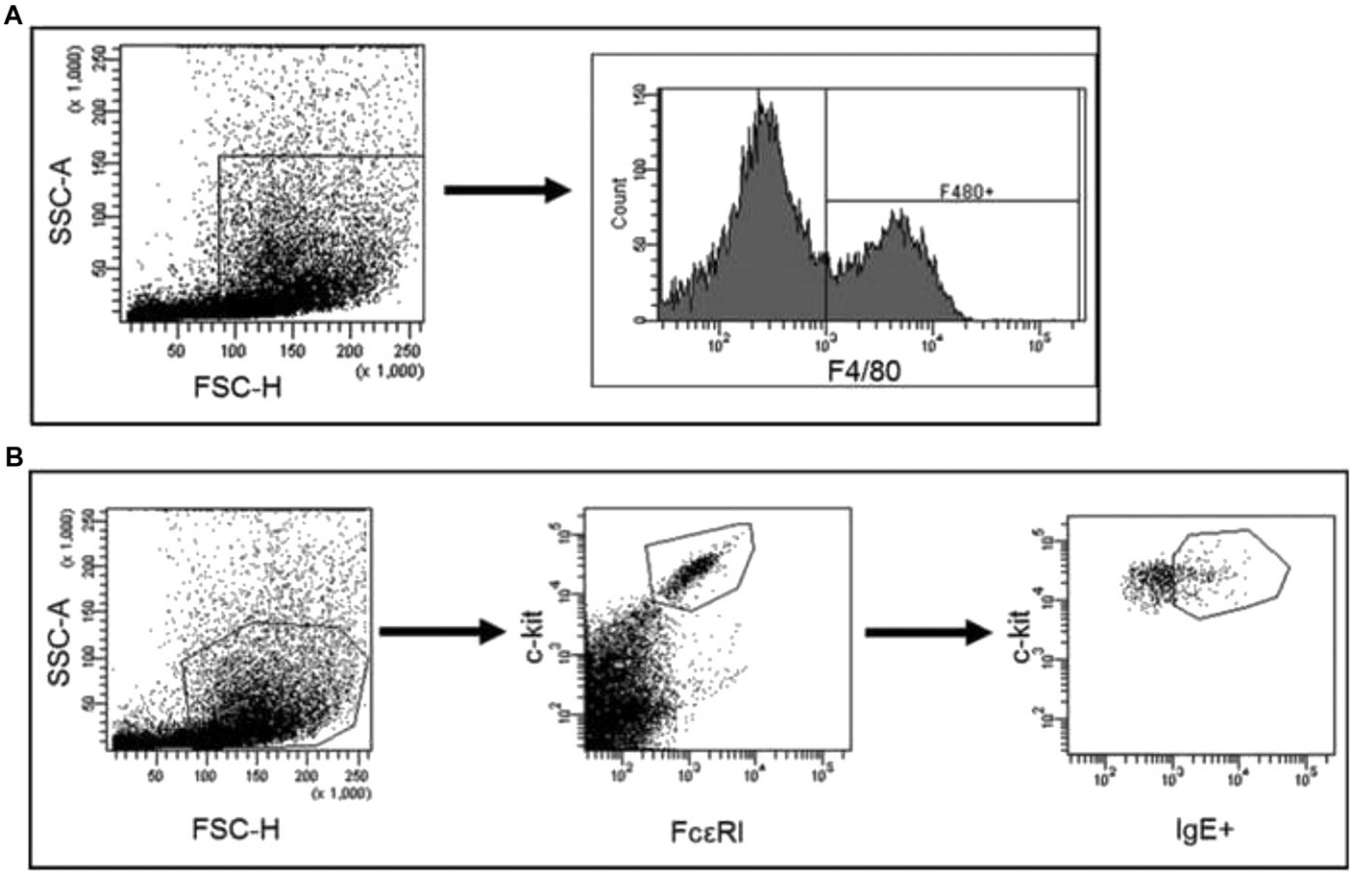

FIG E4. Histograms showing the gating strategy used to identify macrophages **(A)** and MCs **(B)** in whole-lung homogenates by using flow cytometry. *FSC*, Forward scatter; *SSC*, side scatter.

TABLE E1. Primers used for qPCR analyses

Primer	Nucleotide sequence
Cxcl1 forward	5′-GCTGGGATTCACCTCAAGAA-3′
Cxcl1 reverse	5′-CTTGGGGACACCTTTTAGCA-3′
HPRT forward	5′-AGGCCAGACTTTGTTGGATTTGAA-3′
HPRT reverse	5′-CAACTTGCGCTCATCTTAGGCTTT-3′
IFN-γ forward	5′-GAGGAACTGGCAAAAGG-3′
IFN-γ reverse	5′-TTGCTGATGGCCTGATTGTC-3′
IL-1β forward	5′-TGGGATCCTCTCCAGCCAAGC-3′
IL-1β reverse	5′-AGCCCTTCATCTTTTGGGGTCCG-3′
IL-6 forward	5′-AGAAAACAATCTGAAACTTC CAGAGAT-3′
IL-6 reverse	5′-GAAGACCAGAGGAAATTTTCAATAGG-3′
IL-10 reverse	5′-GCCTTGTAGACACCTTGGTCTTGG-3′
IL-13 forward	5′-CAGCCTCCCCGATACCAAAAT-3′
IL-13 reverse	5′-GCGAAACAGTTGCTTTGTGTAG-3′
mMCP-6 forward	5′-CATTTCTGCGCGCAGGTTCTCTC-3′
mMCP-6 reverse	5′-CACCACGATCCTGTTCAAAGA-3′
TNF-α forward	5′-TCTGTCTACTGAACTTCGGGGTGA-3′
TNF-α reverse	5′-TTGTCTTTGAGATCCATGCCGTT-3′

HPRT, Hypoxanthine-guanine phosphoribosyl transferase.